

PROJECTILE FRAGMENTATION AT FERMI ENERGIES WITH TRANSPORT SIMULATIONS

T. I. Mikhailova^{a, 1}, *B. Erdemchimeg*^{a,b}, *A. G. Artukh*^a,
S. M. Lukyanov^a, *Yu. M. Sereda*^{a,c}, *M. Di Toro*^d, *H. H. Wolter*^e

^a Joint Institute for Nuclear Research, Dubna

^b National University of Mongolia, Ulaanbaatar

^c Institute for Nuclear Research, NAS, Kyiv

^d National Laboratory of the South, INFN, Catania, Italy

^e Faculty of Physics, University of Munich, Garching, Germany

Projectile fragmentation at Fermi energies is an important method to produce radioactive beams for the study of isospin asymmetric nuclear matter. Fragmentation is usually successfully parametrized by empirical phase space models. In this contribution we apply a microscopical method, semiclassical transport theory, to study in detail the reaction mechanism of the fragmentation process. We apply it to the experimental data of ^{18}O on ^{181}Ta at $E/A = 35$ MeV measured at FLNR, JINR (Dubna). We consistently calculate the excitation energy of the primary fragments and take into account their decay by a statistical model. It is found that the dissipative part of the fragment spectra is well described by transport theory. However, there are, in addition, important direct and collective contributions.

Фрагментация налетающего иона при энергиях Ферми является важным способом получения пучков радиоактивных ионов для изучения изоспиновой асимметрии ядерной материи. Для параметризации фрагментации успешно используются эмпирические модели фазового пространства. В данной работе мы применяем полуклассическую транспортную теорию, хорошо опробованную при более высоких энергиях для исследования ядерного уравнения состояния. Данный микроскопический подход позволит нам изучить в деталях механизм реакции фрагментации. Мы применяем его для описания экспериментальных характеристик реакции ^{18}O на ^{181}Ta при энергии $E/A = 35$ МэВ, а именно изотопных и скоростных распределений, измеренных под нулевыми углами в Лаборатории ядерных реакций ОИЯИ (Дубна). Мы вычисляем согласованно энергию возбуждения первичных фрагментов и учитываем их распад в статистической модели. Мы находим, что диссипативный спектр фрагментов хорошо описывается в транспортной теории. Тем не менее имеется дополнительный вклад прямых и коллективных процессов.

PACS: 29.38.-c

Beams of unstable nuclei are of great interest today for the investigation of nuclear matter with extreme isospin, for the understanding of astrophysical objects like neutron stars and supernovae, and for fusion reactions leading to production of superheavy elements. One of the preferred methods to produce such beams is projectile fragmentation both at low and at

¹E-mail: tmikh@jinr.ru

relativistic energies [1]. In the Fermi energy regime, in which we are interested here, the mechanism can be seen as an abrasion process followed by de-excitation (ablation) of the fragments, or as deep-inelastic or dissipative collisions with possibly some contribution of quasi-elastic processes. Correspondingly, different methods have been used to describe these processes, such as empirical fragmentation models (EPAX [2]), abrasion-ablation models [3], or phase space parametrization models (HIPSE [4]). While these approaches are largely empirical, they are very efficient to predict fragments yields. Less frequently semiclassical transport model approaches have been used [5–8]. They describe a heavy-ion collision by dissipative mean field dynamics and were very successful at higher energies for the investigation of various aspects of the nuclear equation of state. The advantage of such an approach is that it is based on more fundamental nuclear physics input, such as the mean fields and the effective NN cross sections, and one may study the dependence on these physical quantities. It also allows one to inspect and control in detail the evolution of the collision and, thus, to study the mechanism of the fragmentation process. It is of interest to understand which parts of the process are described by dissipative collisions dynamics and which ones are due to other mechanisms.

We briefly review the transport approach and apply it to interpret experimental data of isotope distributions and velocity spectra measured at FLNR (Dubna) with the COMBAS forward spectrometer [9]. Relative to previous studies of such reactions [6–8], we present here a more consistent calculation of the excitation energies of the primary fragments, which are important for their de-excitation and the final fragments yields. For this comparison the velocity spectra are particularly interesting, since they show other contributions than those described by the dissipative transport theory.

We first give a brief description of the transport approach used in this work. The Boltzmann–Nordheim–Vlasov (BNV) transport approach describes the time evolution of the one-body phase space distribution function $f(\mathbf{r}, \mathbf{p}, t)$ under the influence of a Vlasov self-consistent mean field $U([f(\mathbf{r}, \mathbf{p}, t)])$ and a Boltzmann two-body collision term, which includes the effect of Pauli blocking (Nordheim or Uehling–Uhlenbeck collision term) [10].

$$\begin{aligned} \frac{\partial f_1}{\partial t} + \frac{\mathbf{p}}{m} \nabla_{\mathbf{r}} f_1 - \nabla_{\mathbf{r}} U \nabla_{\mathbf{p}} f_1 = & \left(\frac{2\pi}{m} \right)^3 \times \\ & \times \int d\mathbf{p}_2 d\mathbf{p}_3 d\mathbf{p}_4 |v_1 - v_2| \sigma_{NN}(\Omega_{12}) \delta(\mathbf{p}_1 + \mathbf{p}_2 - \mathbf{p}_3 - \mathbf{p}_4) (f_3 f_4 \bar{f}_1 \bar{f}_2 - f_1 f_2 \bar{f}_3 \bar{f}_4). \end{aligned} \quad (1)$$

Here $f_i = f(\mathbf{r}, \mathbf{p}_i, t)$, $\bar{f}_i = (1 - f_i)$, v_i are velocities and $\sigma_{NN}(\Omega)$ are the in-medium NN cross sections. The potential $U(f)$ used in our calculations is the sum of an isoscalar mean field potential of the Skyrme type [4], a symmetry potential, and the Coulomb potential. The solution of these nonlinear integro-differential equations is achieved by simulations using the test-particle method (more details can be found in [10, 11]).

The time evolution of the reaction is followed until the freeze-out time, which we define as the minimal time when different fragments are sufficiently isolated from each other so that nuclear forces between them are negligible. In these peripheral reactions this is in the range of 100–200 fm/c, depending on the impact parameter. At freeze-out the state of the system can be characterized as a collection of primary fragments with different A and Z , positions, momenta, and intrinsic energy E_{in} . In the systems investigated here, there is usually one heavy projectile-like fragment and one or several lighter ones. Consistent with the transport

calculation, we calculate the intrinsic energy of each fragment E_{in} using the same energy functional that determines the potential U in the transport equation. Thus, we use a consistent treatment of the reaction evolution and the excitation energy calculation, which is a new feature of the present approach. Further, one has to apply a cluster recognition algorithm to identify the fragments. Here we used a simple density cut-off method in coordinate space, so that all test-particles inside a contour of a cut-off density constitute a fragment.

The projectile fragments produced in the transport calculation at the freeze-out configuration are still considerably excited; i.e., the intrinsic energy of the fragment is higher than the ground state energy E_{ground} , calculated for an isotope with the same values of A and Z

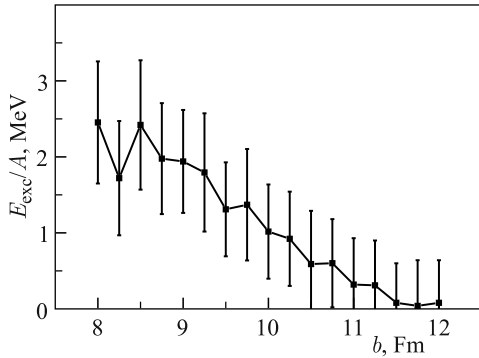


Fig. 1. Mean excitation energy per nucleon (and statistical variance) for the reactions ^{18}O on ^{181}Ta as a function of the impact parameter b

propagated freely until $t = t_{\text{freeze-out}}$ without a reaction. Then we calculate the excitation energy of the fragment as $E_{\text{exc}} = (E_{\text{in}} - E_{\text{ground}})$. The mean excitation energy per nucleon and its statistical variance are shown for the projectile fragment for the reaction ^{18}O on ^{181}Ta at $E/A = 35$ MeV in Fig. 1 as a function of the impact parameter b . One can see that the excitation energy calculated microscopically from the transport model rises slowly with decreasing impact parameter similar as in [5] and in contrast to empirical models, as, e.g., [12]. The excited fragments at freeze-out will de-excite by evaporating further particles and by gamma emission before detection. This secondary evaporation consid-

erably changes the final isotope distributions and velocity spectra and has to be taken into account when compared to experimental data. We use the Statistical Multifragmentation Model (SMM) by Bondorf, Mishustin, and Botvina [13] to treat this de-excitation. Besides the mass and charge of the primary fragment, this model critically uses its excitation energy.

Results of the calculation for isotope distributions of elements at and below the projectile are shown in Fig. 2, and for velocity distributions for one of the more abundant isotopes of these elements in Fig. 3 in comparison with experimental data from [9]. The experimental data are shown as open squares, while the “dissipative part” of the data, which is explained below, is shown as full squares. The results of the BNV transport calculations are shown as open triangles, while the results after de-excitation (SMM) are given by full triangles. Since the experiment did not determine absolute cross sections, the calculations are normalized by a common factor by normalizing the SMM results to the dissipative part of the data for ^{15}N .

One can see that O-isotopes heavier than ^{18}O or ^{18}N are observed experimentally, which correspond to the pickup of nucleons from the target. Also, in the velocity distributions, velocities larger than the beam velocity are observed. It shows that the mechanism of the reaction is not purely dissipative, which would always lead to the loss of mass and energy. Thus, there are important direct contributions such as pickup of nucleons, which is poorly described by transport calculations. In order to compare the calculations with the data, one has to separate, in some way, the direct and dissipative components of the data. We do it in the following empirical way [6]: we fit the velocity spectra above the beam velocity by

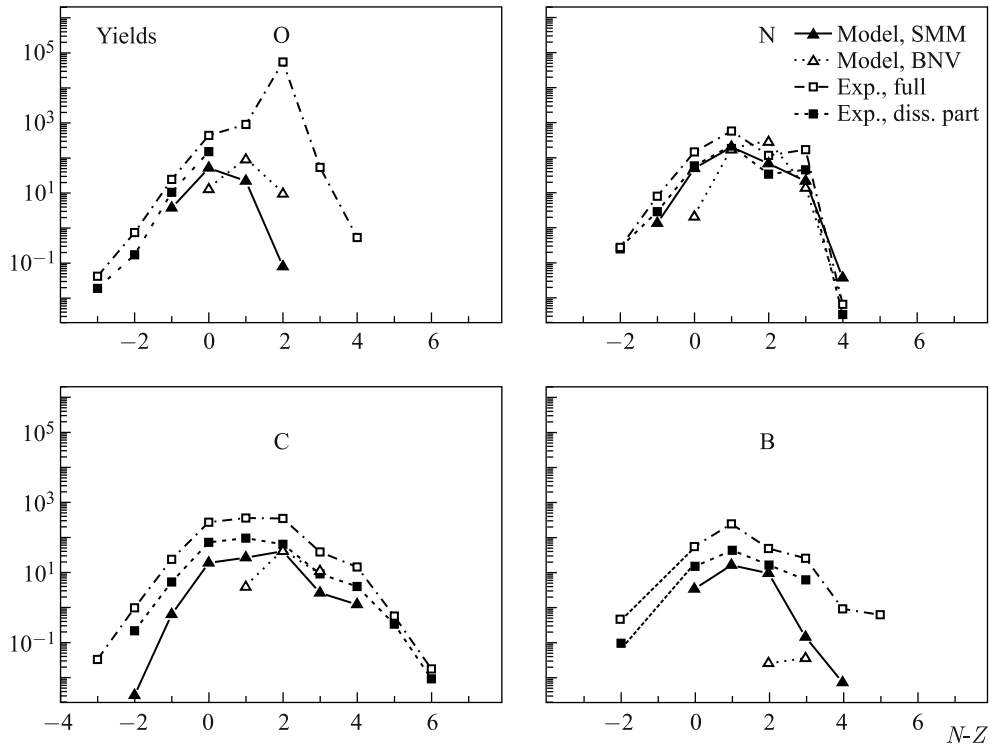


Fig. 2. Isotope distribution for elements at and below the projectile for the reaction ^{18}O on ^{181}Ta at $E/A = 35$ MeV. Experiment [9]: full (open squares), dissipative part (full squares); calculations: primary fragments (BNV, open triangles), after de-excitation (SMM, full triangles)

a Gaussian with the center at the maximum velocity and adjusted width. We then subtract the complete Gaussian from the experimental velocity spectra. We call the remaining part the “dissipative part” of the data, which is shown in Fig.3 by full squares. The integrated dissipative velocity spectra then give the dissipative part of the isotope yields shown in Fig. 2.

As discussed above, the fragments produced in the calculations are still excited and decay by particle and gamma emission. We calculate the excitation energy as discussed above within a consistent description and use the SMM code to de-excite the primary fragments. For the N and C isotopes and the ^{15}N and ^{14}C velocity spectrum the primary (i.e., BNV) distributions are also shown. One can see that the secondary decay essentially changes the distributions and is thus important to make a meaningful comparison to the data. The de-excited distributions (solid triangles in Figs.2 and 3) are then to be compared to the dissipative parts of the data.

One can see that the isotope distributions agree in shape with the data rather well, while the magnitudes are not quite in agreement, which can be improved by a more consistent normalization. The calculated SMM velocity distributions agree fairly well with the dissipative part of the data for velocities around the beam velocity. From this the agreement of the shape of the isotope distributions is natural since these receive their largest contributions from around the beam velocities. However, the calculated spectra for lower velocities, i.e., higher energy loss, decay like a Gaussian, while the experimental data decay exponentially. It seems to point

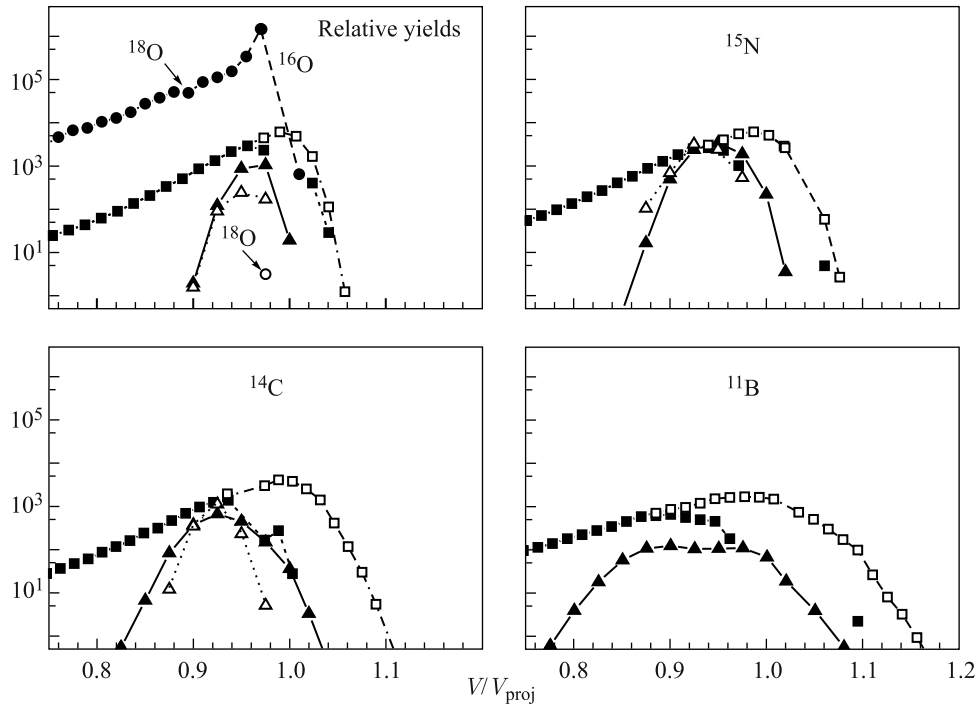


Fig. 3. Velocity distributions for one of the more abundant isotopes for the same reaction as in Fig. 2. The symbols are also the same. For the projectile ^{18}O the velocity distribution for the full experiment (full circles) and the SMM calculation (open circle) are also given

to another mechanism or experimental feature. This is shown particularly clearly for the ^{18}O spectra (see Fig. 3, top left panel). While the calculated spectrum consists essentially of one point close to beam velocity, the experimental spectrum has a long quasi-exponential tail for lower velocities. Such exponential tails were also shown in the work of Borel et al. [14] for similar energies and projectiles. On the other hand, they are not seen in Ar + Ta collisions at the higher energy of 57 MeV/A in the work of Zhang et al. [12]. In [14] they were explained by multiple phonon excitation in the initial phase of the collision leading to energy loss. It is expected that such a process would decrease in importance at higher energies. In any case, it is clear that the transport calculation will not be able to describe such a collective excitation.

Besides this contribution, it would also be desirable to have a more theoretical understanding of the “direct part” of the experimental distribution. It has been interpreted in the Goldhaber picture as a fast breakup of the projectile [15]. In such a picture the width of this component reasonably follows the systematics of the Goldhaber model [8]. However, it has to be clarified how much of such a mechanism is already contained in the transport approach.

To sum it up, we have undertaken a detailed study of projectile fragmentation in a transport approach. A particular feature of this work is the calculation of the excitation energy of the primary fragment consistently with the reaction calculation. It allows us to investigate which parts of the fragmentation reaction are due to dissipative dynamics and where there are other contributions. For this study the velocity spectra are particularly illuminating. One can

see that the transport calculations agree well with the estimated dissipative part of the data. However, there are additional contributions both at higher velocities, most likely as direct breakup or multinucleon transfer processes, and at lower velocities, perhaps due to multiple collective excitations in the initial state. It is desirable to study both these contributions microscopically as well.

This work was supported in part by a grant of the Heisenberg–Landau program of the German DFG, grant No. HLP-2013-24.

REFERENCES

1. *Sherril B. M.* // Prog. Theor. Phys. 2002. V. 146. P. 60.
2. *Sümmerer K., Blank B.* Modified Empirical Parametrization of Fragmentation Cross Sections // Phys. Rev. C. 2000. V. 61. P. 034607.
3. *Bowman J. D., Swiatecki W. J., Tsang C. F.* LBL Report LBL-2908. 1973.
4. *Lacroix D., Lauwe A. V., Durand D.* Event Generator for Nuclear Collisions at Intermediate Energies // Phys. Rev. C. 2004. V. 69. P. 054604-1–054604-12.
5. *Mocko M. et al.* Transport Model Simulations of Projectile Fragmentation Reactions at 140 MeV/Nucleon // Phys. Rev. C. 2008. V. 78. P. 024612-1–024612-12.
6. *Mikhailova T. I. et al.* Fragment Production in Peripheral Heavy-Ion Collisions at Fermi Energies in Transport Models // Intern. J. Mod. Phys. E. 2010. V. 19. P. 678–684.
7. *Erdemchimeg B. et al.* Dissipative Processes in $^{18}\text{O} + ^9\text{Be}$ and $^{18}\text{O} + ^{181}\text{Ta}$ Reactions at Fermi Energies // Nucl. Phys. At. Energy. 2010. V. 11. P. 394–399.
8. *Mikhailova T. I.* Dissipative Processes in Peripheral Heavy-Ion Collisions at Fermi Energies // Bull. Rus. Acad. of Sci. Physics. 2011. V. 75. P. 1511–1516.
9. *Artukh A. G. et al.* Some Regularities in the Beam-Direct Production of Isotopes with $2 < ZZ < 11$ Induced in Reactions of ^{18}O (35A MeV) with Be and Ta // Nucl. Phys. A. 2002. V. 701. P. 96–99.
10. *Bertsch G. F., Das Gupta S.* A Guide to Microscopic Models for Intermediate Energy Heavy-Ion Collisions // Phys. Rep. 1988. V. 160. P. 189–233.
11. *Baran V. et al.* Reaction Dynamics with Exotic Nuclei // Phys. Rep. 2005. V. 410. P. 335–466.
12. *Zhang X. H. et al.* Projectile Fragmentation Reactions of ^{40}Ar at 57 MeV/Nucleon // Phys. Rev. C. 2012. V. 85. P. 024621-1–024621-9.
13. *Bondorf J. P. et al.* Statistical Multifragmentation of Nuclei // Phys. Rep. 1995. V. 257. P. 134–221.
14. *Borel M. et al.* Projectile-Like Fragment Production in Ar Induced Reactions around the Fermi Energy // Z. Phys. A. 1986. V. 324. P. 217–225.
15. *Goldhaber A. S.* Statistical Models of Fragmentation Processes // Phys. Lett. B. 1974. V. 53, No. 4. P. 306–308.